ARTICLE https://nhsjs.com/

An Overview of Carbon Capture and Utilization via Inorganic Catalysis

Aden S. Hwang

Received December 27, 2024 Accepted August 11, 2025 Electronic access September 30, 2025

The mitigation of global warming and climate change are significant issues that must be tackled and which will otherwise lead to destruction across the globe. One of the main causes of this is the rampant emission of CO_2 , making up near 76% of all greenhouse gas emissions. Carbon Capture and Utilization (CCU) is a leading method in combating the rising emissions of CO_2 . As different methods can change the output and outcome of carbon utilization, various catalysts must be considered to maximize the output. Inorganic catalysts, in particular, stand out as their properties allow for more recyclability and stability over time. For example, metal oxides have shown CO_2 adsorption capabilities up to 9.77 mmol/g and enhancement of CO_2 conversion to CO by 97% faradaic efficiency. Photocatalysts such as Ru(bpy) show high CO_2 reduction selectivity, and metal organic frameworks such as HKUST-1 showed CO_2 capture efficiencies of up to 7.52 mmol/g. Despite these capabilities, problems lie in the cost, scalability, and energy requirements, calling for more technological development. This review will assess the synthesis, capabilities, and applications of metal oxides, photocatalysts, and metal organic frameworks as inorganic catalysts in Carbon utilization processes.

Keywords: Chemistry, Environmental Chemistry, Inorganic Chemistry, Inorganic Catalysts, Carbon Capture Utilization and Storage

Introduction

A direct consequence of burning fossil fuels is the excessive levels of CO_2 released, driving global warming and climate change. This generation of CO₂ constitutes nearly 76% of global greenhouse gas emissions ¹. Data collected by NASA show that the past ten years have been the warmest years on record. When compared with 2014, which saw an increase in global temperatures of 0.74 °C relative to a benchmark of the 1950-1981 average, the temperature increase in 2023 was measured at 1.17 ${}^{\circ}C^2$. Droughts, floods, heat waves, and other extreme weather events are amplified by this rise in temperature³. It may be difficult, however, to fully greenify or electrify specific industries such as oil and gas as they require the powerful capabilities of fossil fuels to produce their energy-intensive processes⁴(. As such, capturing released carbon and repurposing it creates an efficient and sustainable way to slow down the rise in CO_2 levels and protect the environment. This strategy, better known as Carbon Capture, Utilization, and Storage (CCUS), is a promising solution.

Through various methods, CCUS + 63 can be used to safely and efficiently store emissions, and create products with an already existing market. In particular, methanol and urea are common products of CCUS. Enhanced oil recovery and conversion into biochar are also popular processes, contributing to agriculture and fuel production.

The first step in the CCUS process is carbon capture. As advancements in strategies for CO_2 capture have gained increasing global prominence in the past two decades, the technology has favored point sources where CO_2 is highly concentrated⁵. Point-source capture refers to methods in which CO_2 is extracted before the release of the other fuel consumption byproducts, namely through pre-combustion, oxyfuel combustion, or direct air capture. However, broader issues across the entire process hinder its viability on an industrial scale.

CCUS processes is currently held back by its developing technology, especially within infrastructure for storing and transporting carbon, as well as a need for sustainable sources of energy 6 . Due to this, CCUS currently lacks scalability in terms of cost and efficiency. Furthermore, CO_2 must undergo purification and transportation prior to utilization, requiring development in those fields alongside utilization for a more cohesive development.

Incorporating catalysts is an essential step in scaling CCUS to an industrial level. As discussed earlier, for CCUS to be improved, other fields such as carbon storage and transport both need to be developed further. As such these inorganic catalysts can assist in CCUS. By introducing catalysts into CCUS processes, they assist with the adsorption and conversion of CO_2 into value-added products. In storage, inorganic catalysts can adsorb CO_2 through their distinct porous structures and surface modifications. In utilization, catalysts lower the activa-

tion energy required to convert the CO_2 into useful chemicals. Inorganic catalysts are gaining significant attention for their potential in CO_2 capture, owing in part to their intrinsic properties, including porosity and solubility, which may hold significance in creating a greener future. Industrial leaders are already utilizing CO_2 and inorganic catalysts in order to create products such as ethylene and polyols, which are then used to replace fossil fuels 7,8 .

This review focuses specifically on inorganic catalyst. Unlike homogeneous or enzymatic systems, they show capabilities in cost-effectiveness, thermal stability, recyclability, and potential for larger scale application.

Current studies have highlighted various categories and specific catalysts for CCUS. However, few provide a cohesive view and comparison of various inorganic catalysts and their performance. This review will delve into the synthesis, properties, and applications of metal oxides, photocatalysts, and metal-organic frameworks (MOFs) in CCUS, to assess their development, broader applicability, and potential environmental impact.

Methodology

To compile information and data for this review, an extensive search was taken to gather relevant and recent information regarding carbon capture and inorganic catalysis. In particular, sources were chosen from peer-reviewed, high-impact journals from Google Scholar in order to ensure the credibility of the information presented. Sources detailing advancements from the past 20 years were prioritized in order to use the most up-to-date information for the review.

Furthermore, data extraction was conducted with the following keywords: catalysis, CO_2 conversion, MOFs in CO_2 reduction, photocatalytic CO_2 reduction, etc. By using these keywords, sources were narrowed down to be most relevant towards addressing the role of inorganic catalysts in CCUS.

Discussion

Inorganic Catalysts

The relative inertness of CO_2 (bond dissociation energy of around 1600 kJ/mol) often requires catalysts to help break the covalent bonds⁹. Inorganic catalysts show great promise in carbon capture and conversion due to their stability in harsh environments and high turnover numbers. As carbon capture and conversion typically go hand in hand, this section will discuss the development of inorganic catalysts and their applications to both processes.

A common process used in developing inorganic catalysts is sol-gel, a wet chemical method used for the synthesis of nanostructures ¹⁰. By dissolving a molecular precursor, turning it into a gel, and then drying it, materials such as metal oxides

can be synthesized ¹⁰. Another method is solvothermal synthesis, which is conducted under high pressure and creates high-quality crystalline structures ^{11,12}. In this process, a new material is produced by placing a precursor and solvent in a closed system in which the temperature rises beyond the boiling points of the solvent ¹³.

The optimization for certain traits is essential in the synthesis of catalysts. For CCUS, surface area, porosity, and water solubility are critical considerations, as they affect the way the catalysts absorb and adsorb CO_2 . Catalyst sustainability, either in turnover number or the availability of the material itself, is also an important consideration in maximizing the environmental benefits. Additionally, it is also important to consider the identity and associated properties of the catalyst, which can help maximize efficiency and meet targets, such as environmental impact thresholds. The following sections will examine what properties are associated with various catalysts among metal oxides, photocatalysts, and metal-organic frameworks.

Metal Oxides

A metal oxide is a compound with a metal cation and oxygen anions, mainly in the form of ionic bonds. These have been studied since the 1950s for hydrocarbon processing, in which hydrocarbons are converted into valuable products, and for their oxidizing capabilities ¹⁴. They are studied so often in part of their Unlike other catalysts, such as zeolites and activated carbons, metal oxides exhibit high thermal stability and high selectivity under harsh conditions ¹⁵. Additionally, metal oxides' intrinsic reactivity with CO2 makes them an attractive option for capture and conversion. Furthermore, they are more cost-effective than many catalyst alternatives and are also less toxic ¹⁶. The reactions catalyzed by metal oxides can be further improved by implementing supporters such as silicas and aluminas, providing better stability for the catalysts ^{17,18}. However, a key limitation with widespread metal oxide implementation in CCUS is the high consumption of energy required to activate and in each catalyst turnover, which is correlated with their fast-saturating properties and raises questions of sustainability ^{15,19}.

a. Magnesium Oxides

Magnesium oxide (MgO) is particularly useful in performing CO_2 absorption, a type of CO_2 capture in which CO_2 is selectively dissolved from a gas mixture. MgO's surface morphology is suitable for oxygen generation, resulting in efficient CO_2 absorption and low energy consumption for regeneration 20 . Activating carbon nanofibers with MgO generates a catalyst capable of increasing CO_2 absorption capacity up to 2.72 mmol/g²¹. Supporting activated carbon-based bamboo (BAC) using MgO nanoparticles (NPs) also shows strong adsorption capabilities. Relative to the physical absorption of regular BACs (18.8 mg/g),

the MgO(NPs)-BAC (39.8 mg/g) showed a 112% increase in the physical adsorption of CO_2^{22} . Furthermore, fibrous silicas can be improved using MgO. Regular fibrous silicas show an absorption of CO_2 of 0.52 mmol/g, while MgO-infused fibrous silicas have an absorption of 9.77 mmol/g¹⁷.

b. Calcium Oxides

Despite excessive sintering and relative ease of decomposition, calcium oxide (CaO) is an excellent solid adsorbent for CO_2 . CaO nanoparticles derived from nanosized CaCO3 show a 20% increase in the amount of CO_2 converted, relative to bulk CaO ¹⁵. Furthermore, if the CaO is carbonated for a sufficient duration prior to use, the aforementioned drawbacks of sintering and decomposition are significantly reduced ²³. Another study found that a hydrated solution of CaO in a multi solvent mixture of water and ethanol shows a near 100% increase in the catalyst's sorption capacity, and it is theorized that alternative syntheses could further increase catalyst efficiency²⁴. CaO, when dispersed on an inactive support such as -Al2O3, also demonstrates an increase in sorption capacity 25. In comparison to standard CaO, the Al-dispersed CaO showed a higher capacity to bind CO_2 , reduced sintering, and high efficiency in low temperatures, circumventing a traditional limitation of metal oxide catalysts ²⁶. The dispersed CaO also shows long-term stability, maintaining 90% of its efficiency as compared to bulk CaO (at 50%) after 20 cycles^{26} .

c. Zinc Oxides

Five metal oxides (ZnO, SnO2, Fe2O3, La2O3, and CeO2) were tested to see which would have the greatest catalytic effect on the process of transforming glycerol into glycerol carbonate with CO_2 as a reactant (Figure 1)²⁷. Zinc oxide showed the greatest efficiency, yielding 8.1% of glycerol carbonate ²⁸. Furthermore, bimetallic ZnCu electrocatalysts can be used to selectively achieve a highly efficient conversion of CO_2 into CO. While the selectivity of ZnO alone is limited to 30% faradaic efficiency, a measurement of how efficiency charges are transferred in a system during an electrochemical reaction, the two-metal combination increases the selectivity to 97% faradaic efficiency ²⁸. Additionally, a CuO-ZnO-ZrO catalyst supported by graphene oxide (GO) has shown excellent efficiency in converting CO_2 to methanol. The addition of GO (0.5-2.5 wt%) increases the availability of active sites for the adsorption CO_2 and H2, thus increasing selectivity for methanol production from around 70% (without GO) to 75.9% (with GO) and further enhancing the overall yield of methanol²⁹.

d. Nickel

Nickel oxides (NiO) are attractive metal complexes for Carbon utilization, with high reactivity and cost-efficiency. However,

drawbacks include their tendency to sintering at high temperatures and deactivation from coke formation 30 . Ceria has been shown to counteract these limitations by dispersing the NiO over a support framework and reducing sintering, thus enhancing the Ni's performance 31 . Reduced GO-supported NiO shows a 63.1% CO_2 conversion rate, while the addition of ceria increases the rate to 84.5% 32 . NiO nanoparticles themselves are also competent at carbon capture, increasing carbon absorption by 34% in limited-mixing conditions (incompletely mixed) and 54% in high-mixing conditions (completely mixed) 15 .

e. Titanium

 TiO_2 , a porous metal oxide, shows a rate of catalytic conversion of CO_2 up to 10 times higher than methane's, yielding from 2 to 3 times as much CO^{33} . A bimetallic combination of bismuth and titanium (Bi_2O_3 - TiO_2) showed that TiO_2 polymorphs such as rutile and anatase can be modified with this compound to better adsorb CO_2^{34} . Carboxylate production from CO_2 through electron transfer is also made possible through the catalyst's strong adsorption and alteration capabilities 34 . Thus, TiO_2 is a versatile stepping stone to the reductive conversion of CO_2 to other value-added materials.

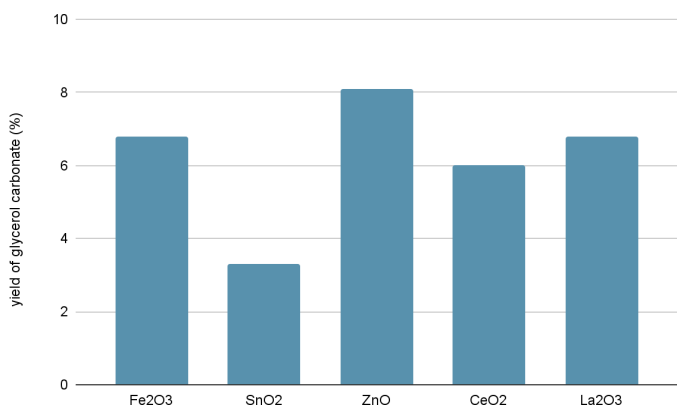


Fig. 1 Comparison of the yield of glycerol carbonate over five metal oxides $(180 \,^{\circ}C, 150 \, \text{bar}, 12 \, \text{hours})^{27}$.

This overview provides a comparison of metal oxides' cost and lifetime in addition to their reactivity and efficiencies presented earlier.

Photocatalysts

Unlike metal oxides, which use heat as a source of activation, photocatalysts are compounds that absorb photons as a means to gather energy and perform redox reactions and/or sensitizations. As a result, photocatalysts provide a more environmentally positive option for CO_2 transformation, gaining attention in recent years as their loadings tend to be significantly lower than those of traditional catalysts. Furthermore, as they are activated by

Table 1 Comparison of Metal Oxides' Lifetime and Cos

	Lifetime	Cost (per
		100 grams)
Magnesium Ox-	Lasts around 10-20 cy-	~\$85
ide	cles ¹⁵	per 100
		grams ³⁵
Calcium Oxide	Lasts over 20 cycles	~\$9
	(when dispersed on -	per 100
	AlO.) ¹⁵	grams ³⁶
Zinc Oxide	Lasts over 25 adsorption-	~50\$
	desorption cycles ³⁷	per 100
		grams ³⁸
Nickel Oxide	Doesn't last long, but	~\$140
	its lifetime can be ex-	per 100
	tended with ceria as a	grams ³⁹
	supporter 15	
Titanium Oxide	Lasts incredibly long	~\$60
	even in sunlight 40	per 100
		grams ⁴¹

light, they do not require harsh or energetically costly conditions (e.g. high temperatures). Solar energy is also a major source of photons, allowing photochemical transformation through this method to have minimal impact on the environment 33 . Furthermore, spatiotemporal control can be achieved with the use of photocatalysis, as the scope of reactivity is localized to the presence of both the light and the catalyst 42 . Photocatalysts are also capable of creating exotic and valuable bond constructions more readily than previously established protocols 43 . However, a clear disadvantage of using photocatalysts is that they can lack substrate selectivity, leading to off-cycle reactivity and low CO_2 reduction 33 . As such, a heavy emphasis in photocatalyst development for CO_2 capture and conversion is on improving yields of and selectivity for the desired product.

a. Re(I)

A commonly utilized metal complex in CO_2 conversion is rhenium(I), which displays high selectivity of products (preferentially forming CO) and reduction efficiency of CO_2^{44} . Rhenium can be utilized through Re(bpy)(CO)3L complexes, where L is an X-type ligand, typically -NCS, -Cl, or -CN⁴⁴. The NCS complex is the most efficient, producing around 60 μ Mol of CO after 25 hours of irradiation, while the -Cl complex produces half of that amount ⁴⁴. All three examples also show the highest efficiency between 300 and 400 nm (UV) irradiation ⁴⁴. In a DMF-triethanolamine solvent system, the production efficiency and selectivity of CO are increased ⁴⁵. Furthermore, adding bromide or chloride counterions can increase the durability of the complex. This prevents the formation of formate complexes,

which can lower the CO_2 reduction efficiency ⁴⁵. However, one significant drawback of widespread Re(I) adoption is the toxicity associated with the CO ligands. Further development and addressing this issue may make Re(I) complexes even more prominent.

b. $(GO) - TiO_2 - Ag_2O$ (with or without Arg)

GO, when combined with TiO_2 , a semiconductor used for CO_2 reduction, possesses considerable absorption and a large conductivity capacity (5000 W m-1 K-1), creating a versatile composite 46 . Adding silver oxide (Ag_2O) allows the catalyst to surpass TiO_2 's catalytic limitations ⁴⁷. The energy gap between this photoactive composite's ground and excited states can be bridged with high-energy UV light with excellent efficiency⁴⁷. Adding arginine (Arg) as a sacrificial agent increases the catalyst's overall efficiency and the photoluminescence (PL) absorption surface, red-shifting its absorbance wavelength to the visible light region 47 . $GO - TiO_2 - Ag_2O - Arg$ shows higher absorption of CO_2 than $GO - TiO_2 - Ag_2O$ under most conditions, aside from irradiation under UV light at 40 $^{\circ}$, where $GO - TiO_2 - Ag_2O$ outperforms the Arg-modified catalyst by about 300 mmol/g (Table 1)⁴⁷. Under UV and visible light, respectively, $GO - TiO_2 - Ag_2O$ produces 32.616 $\mu mol/g$ catalyst of methanol, and GO- $TiO_2 - Ag_2O - Arg$ produces 20.385 \(\mu mol/g\) catalyst of methanol over 4 hours, outperforming the yields of comparable photocatalysts (Table 2)^{47–54}. When reused, both composites lose little efficiency, suggesting that they may be sustainably viable ⁴⁷.

c. Ru(bpy)

The photocatalyst $[Ru(bpy)(CO)_2Cl_2]$ (and its reduced form, $[Ru(bpy)(CO)_2]^{2+}$) excels at the conversion of CO_2 into CO and formic acid via a multi-step photo-electrocatalytic cycle. When combined with a nitrogen doped Ta2O5 semiconductor, the complex acts as a charge-transfer mediator between the photosensitizer and CO_2 . In these conditions, its performance increases dramatically, showing turnover numbers less than 10 as well as a redox potential of 0.7 V vs. SHE⁵⁵. When in contact with light, electrons from the semiconductor are transferred to the Ru-complex. Through sequential two-electron reduction, the hydride complex $[Ru(bpy)_2(CO)H]^+$ is created, which takes in CO_2 , and eventually creates formic acid, after which the cycle renews 55. With a free energy of 18.56 kcal mol-1 and an activation energy of +32.91 kcal mol-1, the cycle is accessible both kinetically and thermodynamically 55. The selective product formation and absorption of light makes Ru- based complexes promising for CO₂ conversion. However, as its precursor utilizes a rare metal and released carbon monoxide in its cycle, its potential usage is hindered by its economical viability and environmental impact⁵⁵.

Table 2 Comparison of CO_2 absorption capacity of catalysts in various conditions (10 bar)⁴⁷.

	Catalyst	Temp (°C)	Light	CO ₂ ab-
				sorption
				(mmol/g)
1	$GO - TiO_2 -$	r.t.	UV	1237.815
	Ag_2O-Arg			
		40	UV	690.27
İ		r.t.	visible	1255.461
İ		40	visible	786.544
2	$GO - TiO_2 -$	r.t.	UV	1209.27
	Ag_2O			
		40	UV	988.695
		r.t.	visible	1183.32
		40	visible	621.502

This table compares the CO_2 absorption efficiencies of various photocatalysts under different light conditions.

Table 3 Comparison of Catalyst Activity in Synthesis of Methanol (CH3OH) from $CO_2^{47-54,56}$.

	Catalyst (g)	Reaction	Product
		condition	$(\mu mol/g$ cata-
		light / time	lyst)
		(hr)	
1	$V - TiO_2 (0.2)$	Visible/4	CH ₃ OH (4.6)
	$Cr - TiO_2$ (0.2)		CH ₃ OH (2.94)
	$Co-TiO_2$ (0.2)		CH ₃ OH (6.53)
2	$Ag-TiO_2$ (0.1)	UVVisible/8	CH ₃ OH (29)
		and 6	
			CH ₃ OH (15)
3	N-doped TiO ₂	UVVisible/2	CH ₃ OH (20)
	(0.6)		
4	$NTiO_2(0.1)$	Visible/2	CH ₃ OH (0.2)
5	$FeTiO_3/TiO_2$	UVVisible/3	СН3ОН
	(0.05)		(1.3861.296)
6	Cu/FeTiO ₂ -	no h	CH ₃ OH (4.12)
	SiO_2		
7	Ti-silica film	no h	CH ₃ OH (11)
8	$g - C_3 N_3 (0.1)$	UVVisible/1	CH ₄ /CH ₃ OH
			(0.26)
	amine-	UVVisible/1	CH ₃ OH (0.28)
	functionalized		
	$g - C_3 N_4 (0.1)$		
9	$GO - TiO_2 -$	UV/4	СН3ОН
	$Ag_2O(0.1)$		(32.616)
10	$GO - TiO_2 -$	Visible/4	СН3ОН
	$Ag_2O - Arg(0.1)$		(20.385)

This table compares the methanol production efficiencies of various photocatalysts under different light conditions.

Table 4 Comparison of Photocatalysts' Lifetime and Cost.

	Lifetime	Cost
Re(I)	TON of 30 (with 1-NCS) ⁴⁵	∼\$500 per gram
		(precursor) ⁵⁷
(GO) -	Can be reused many times	~\$60 per 100
TiO_2 -	without losing efficiency 47	grams 41
Ag_2O		
Ru(bpy)32+	TON of 4000	~\$278 per
	(with 5.0 μM of	gram ⁵⁸
	$trans(Cl)Ru(bpy)(CO)_2Cl_2)$	

This overview provides a comparison of photocatalysts' cost and lifetime in addition to their reactivity and efficiencies presented earlier.

Metal-Organic Frameworks

Metal-organic frameworks (MOFs) are marked by their highly tunable, lattice-like structures composed of metal nodes and organic linkers, and large surface area, setting them apart from metal oxides and photocatalysts. Furthermore, MOFs contain an extremely high degree of porosity, making them an attractive option for CO_2 capture ⁵⁹. MOFs are also stable, maintaining structural integrity over multiple cycles of use, which contributes to arguments for their sustainability and scalability 60. Their main advantage over other catalysts arises from their ability to be modularized both before and after synthesis. As a result, many of MOFs' structural properties, such as pore size, metal centers, and organic linkers, can be tuned for a specific purpose ⁵⁹. However, the reaction environment may significantly influence their performance and reactivity. Moisture, for example, can decompose the MOFs⁶¹. They are also costly to produce on large scale, and as such, scalability to industrial levels is a significant challenge to be addressed. Despite these limitations, MOFs show potential for their long-lasting lifetime and CCS/CCU efficiency.

a. MOF-808

MOF-808 is composed of hydroxo/aquo-termimated Zr6O8 clusters held together by benzene-1,3,5-tricarboxilate (BTC) ligands ⁶². By binding amino acids to the backbone, different functionalities and qualities of MOF-808 derivatives, such as their regeneration and CO_2 capture efficiency, were tested. Among these amino acids, MOF-808 absorbed the most CO_2 when combined with glycine (15 kPa; 0.693 mmol/g) and DL-lysine (15 kPa; 1.949 mmol/g)⁶³. MOF-808 also possesses interconnected pores of varying sizes, consisting of smaller pores (which are inaccessible to guest molecules) and complementary larger pores,

contributing to the selectivity for CO_2^{63} . The amino groups on alkyl chains are oriented towards these pores, which are the primary sites for CO_2 capture 63 . A vital source of CO_2 is flue gas, which is constituted mainly by CO_2 (8-15%) 64 . In order to capture flue gas at a low cost, MOFs need to be moderately water and moisture-tolerant. MOF-808s have shown retained catalytic behavior under humid conditions, with certain variations such as MOF-808-Gly even enabling an increased CO_2 uptake when in humid conditions 63 . This makes MOF-808 more efficient in an environment where other catalysts may deteriorate, maintaining uptake capacity even after 80 cycles 63 . This implies its sustainability for long-term and widespread usage, as it can operate effectively within a green solvent (i.e. water).

b. MOF-5

MOF-5 is distinguished by its exceptionally stable and porous framework. Its structure is defined by an octahedral array of 1,4-benzene-dicarboxylate (BDC) groups joined with inorganic $[OZn_4]^{6+}$ groups 65. Even when solvent molecules are evacuated, MOF-5s maintain their structure and porosity, emphasizing their potential in CO_2 storage⁵⁹. MOF-5s also contain Zn2+, which harbor defect sites (i.e. crystalline imperfections) that can serve as the active sites for the reaction of CO_2 to epoxides, forming the matching cyclic carbonate ⁶⁶. However, this reaction operates mainly under harsh conditions, requiring high temperatures and pressures ⁵⁹. This suggests that the catalytic activity within defect sites may not produce enough yield to be considered efficient. As such, research aimed towards increasing the density of defect sites is an active area of exploration. Methods such as post-synthetic treatment with acids and bases, as well as using isostructural mixed linkers, have also been explored to increase the performance of MOF-5 and its derivatives ⁶⁷.

c. HKUST-1

HKUST-1, made of copper nodes and connected by benzene-1,3,5-tricarboxilate (BTC) ligands, is characterized by a large surface area and porous structure, characteristic of efficient MOF-based catalysts ⁶⁸. Its structure contains linked cages, one of smaller diameter (3.5) and one larger (9)⁶⁹. The main appeal of HKUST-1 stems from the benefits conveyed by post-synthetic modification using amines. By heating the molecule at 200 C, water is removed, leaving behind coordinatively unsaturated sites (CUS)⁶⁹. Amines, which have a high CO_2 capture yield, are then attached to the CUSs. For instance, Zelenka and colleagues used ethylenediamine (en) and diethylenetriamine (deta) to modify the catalyst⁶⁹. By introducing these amines at different ratios relative to the core MOF structure, they determined which amine loadings result in the greatest yields. At higher MOF to amine ratios (1:2 for en, 1:1.15 for deta), the compound shows signs of decomposing due to the alkaline-dense environment⁶⁹. Further amine loading screens indicate that lower MOF-to-amine ratios are favorable for increasing CO_2 capture⁶⁹. With en, the highest yield of captured CO_2 is 22.31 wt.% (5.07 mmol/g), at a MOF to amine ratio of 1:0.1⁶⁹. With deta, the MOF yields 33.09 wt.% of captured CO_2 (7.52 mmol/g), at 1:0.05⁶⁹. Increasing the ligand size in a HKUST-1 with a copper center shows a decrease in copper density ⁷⁰. While this lowers the MOF's conductivity, it contributes to greater versatility in gas storage ⁷⁰.

Table 5 Comparison of MOFs' Lifetime and Cost.

	Lifetime	Cost
MOF-808	Lasts over 80 vacuum swing	\sim \$866 per kilo-
	adsorption cycles 63	gram ⁷¹
MOF-5	Lasts over 50 adsorption-	\sim \$530 per kilo-
	desorption cycles ⁷²	gram ⁷³ (78.6% of
		the cost is the sol-
		vent)
HKUST-	Lasts over 10 adsorption-	\sim \$70 per gram ⁷⁵
1	desorption cycles 74	

This overview provides a comparison of MOFs' cost and lifetime in addition to their reactivity and efficiencies presented earlier

Challenges and limitations

While inorganic catalysts provide hope in making CCUS more sustainable and viable, the scalability of both the CCUS processes and catalysts remain a large issue. High costs, material scarcity, and threats to the environment stunt the field from growing into an industry-scale process.

Catalysts can be used to make these processes faster, but also suffer from largely the same limitations as conventional methods of CCUS. For example, while Re- and Ru-based photocatalysts have powerful reduction capabilities, they often require expensive and scarce metal precursors (0.7 and 1 ppb in the crust of the earth, respectively)⁷⁶. The scarcity and cost of materials make them hard to bring into an industry scale. Using photocatalysts also comes with dangers. [Ru(bpy)(CO)Cl], contain and release CO, which is highly toxic and hence dangerous to scale up. Furthermore, photocatalysts typically use organic solvents such as DMF, which can only be disposed through storage or burning. While this is passable in a laboratory setting, it's another factor to consider in scaling up catalysts.

CCUS is a great step towards cutting down on carbonemissions, however, as seen by the review, these processes and catalysts typically have a high energy cost, potentially making it less sustainable. Without advancements in catalyst efficiency and renewable energy sources, this process may leave harmful footprints behind its intended purpose of cleaning the environment.

Conclusion

Within CCUS, inorganic catalysts may be a potential solution due to their outstanding efficiency and properties. Three categories of these catalysts have been explored in recent research efforts and are highlighted in this review: metal oxides, photocatalysts, and MOFs.

Metal oxides, including magnesium, calcium, zinc, nickel, and titanium oxides, are highlighted for their strong adsorption capabilities and reactivity with CO_2 . However, some suffer from deactivation and sintering, requiring extra supports to fully utilize their properties. Furthermore, photocatalysts, such as Re(I), $(GO) - TiO_2 - Ag_2O$, and $Ru(bpy)_3^{2+}$, all exhibit highly versatile reactivity alongside their standout ability to utilize solar power. More development and optimization of their properties may modify these catalysts to be more efficient in CCUS. Finally, MOFs, including MOF-808, MOF-5, and HKUST-1, demonstrate excellent modularity and structural efficiency for CCUS. However, they are currently hampered in their high cost and inability to withstand certain reaction conditions.

This technology is still in its early stages of development and requires efficiency, cost, and scalability development. These critical factors must be addressed before the employment of inorganic catalysts in CCUS becomes more widespread. Strides are being taken outside of CCUS to help approach the net zero emissions goal (NZE) by 2050, including growth in sales of electric vehicles and promotion of energy efficiency⁷⁷. However, most of these goals are currently behind target benchmarks and require more intensive efforts to achieve widespread adoption. CCU is one such goal, indicating a call for greater urgency of implementation if the NZE goal is to be achieved. Projections indicate that a successful integration of CCUS technologies may mitigate up to 25.4% of total carbon emissions². Increasing efforts are being invested in the development of these CCUS technologies, and there is hope that CCUS will enable a significant and positive change to how our global society is powered.

Acknowledgments

I would like to extend gratitude to Katherine A. Xie for her mentorship throughout the process of this review.

References

1 Center for Climate and Energy Solutions, Global Emissions, https: //www.c2es.org/content/international-emissions/#: ~:text=by%20Gas%2C%202015-,Notes,are%20expressed% 20in%20C02-equivalents, Accessed: 2024-09-04.

- 2 Power Technology, How is global industry utilising CCUS technologies in 2024?, https://www.power-technology.com/features/how-is-global-industry-utilising-ccus-technologies-in-2024/, Accessed: 2024-09-04.
- 3 NASA, Global Temperature, https://climate.nasa.gov/vitalsigns/global-temperature/?intent=121, Accessed: 2024-09-04.
- 4 NASA, Extreme Weather and Climate Change, https://science.nasa.gov/climate-change/extreme-weather/.
- 5 K. Thambimuthu, M. Soltanieh and J. C. Abanades, Special Report of the Intergovernmental Panel on Climate Change, Cambridge University Press, 2025, pp. 105–178.
- 6 M. J. Regufe, A. Pereira, A. F. P. Ferreira, A. M. Ribeiro and A. E. Rodrigues, Energies, 2014, 14, 2406.
- 7 LanzaTech, LanzaTech Produces Ethylene from CO2, Changing the Way We Make Products Today, https://lanzatech.com/lanzatech-produces-ethylene-from-co2-changing-the-way-we-make-products-today/.
- 8 Covestro, CO2 as a new raw material becoming a jack of all trades, https://www.covestro.com/en/sustainability/what-drives-us/circular-economy/alternative-resources/co2-as-a-raw-material.
- 9 T. P. Minyukova and E. V. Dokuchits, *International Journal of Hydrogen Energy*, 2023, 48, 22462–22483.
- 10 D. Bokov, A. Turki Jalil, S. Chupradit, W. Suksatan, M. Javed Ansari, I. H. Shewael, G. H. Valiev and E. Kianfar, Advances in Materials Science and Engineering, 2021.
- 11 C. M. Gonzlez, E. M. Morales, A. de Tellez, T. E. Quezada, O. V. Kharissova and M. A. Mndez-Rojas, *Handbook of Greener Synthesis of Nanomaterials and Compounds*, 2021, vol. 2, pp. 407–448.
- 12 H. Zhong, T. Mirkovic and G. D. Scholes, Comprehensive Nanoscience and Nanotechnology, 2011, vol. 1-5, pp. 153–201.
- 13 G. Ledoux, M. F. Joubert and S. Mishra, Photonic and Electronic Properties of Fluoride Materials, 2016, pp. 35–63.
- 14 S. Laurent, S. Boutry and R. N. Muller, Iron Oxide Nanoparticles for Biomedical Applications, 2018, pp. 3–42.
- 15 N. H. Khdary, A. S. Alayyar, L. M. Alsarhan, S. Alshihri and M. Mokhtar, Catalysts, 2022, 12, 300.
- 16 A. A. Azmi, A. H. Ruhaimi and M. A. A. Aziz, Materials Today Chemistry, 2016, 16, 100273.
- 17 S. M. Yusof, R. Othaman, H. D. Setiabudi and L. P. Teh, *Journal of Solid State Chemistry*, 2021, 294, 121845.
- 18 B. Alrafei, I. Polaert, A. Ledoux and F. Azzolina-Jury, *Catalysis Today*, 2020, **346**, 23–33.
- 19 S. M. Hashemi, D. Karami and N. Mahinpey, Fuel, 2020, 269, 117432.
- P. Li, R. Chen, Y. Lin and W. Li, Chemical Engineering Journal, 2021, 404, 126459.
- 21 F. E. Othman, N. Yusof, S. Samitsu, N. Abdullah, M. F. Hamid, K. Nagai, M. N. Abidin, M. A. Azali, A. F. Ismail, J. Jaafar, F. Aziz and W. N. Salleh, *Journal of CO2 Utilization*, 2021, 45, 101434.

- 22 W. N. Wan Isahak, Z. A. Ramli, M. W. Mohamed Hisham and M. A. Yarmo, 43 C. K. Prier, D. A. Rankic and D. W. MacMillan, Chemical Reviews, 2013, AIP Conference Proceedings, 2013, pp. 882-889.
- 187-191.
- 24 Y.-J. Li, C.-S. Zhao, C.-R. Qu, L.-B. Duan, Q.-Z. Li and C. Liang, Chemical Engineering & Technology, 2008, 31, 237-244.
- 25 A. A. Belova, T. M. Yegulalp and C. T. Yee, Energy Procedia, 2009, 1, 749–755.
- 26 M. S. Duyar, R. J. Farrauto, M. J. Castaldi and T. M. Yegulalp, Industrial & Engineering Chemistry Research, 2013, 53, 1064–1072.
- 27 L. P. Ozorio and C. J. Mota, ChemPhysChem, 2017, 18, 3260-3265.
- 28 L. Wang, H. Peng, S. Lamaison, Z. Qi, D. M. Koshy, M. B. Stevens, D. Wakerley, J. A. Zamora Zeledón, L. A. King, L. Zhou, Y. Lai, M. Fontecave, J. Gregoire, F. Abild-Pedersen, T. F. Jaramillo and C. Hahn, Chem Catalysis, 2021, 1, 663–680.
- 29 T. Witoon, T. Numpilai, T. Phongamwong, W. Donphai, C. Boonyuen, C. Warakulwit, M. Chareonpanich and J. Limtrakul, Chemical Engineering Journal, 2018, 334, 1781-1791.
- 30 R. Zhang, K. Lu, L. Zong, S. Tong, X. Wang, J. Zhou, Z.-H. Lu and G. Feng, Molecular Catalysis, 2017, 442, 173–180.
- 31 Z. Qin, J. Ren, M. Miao, Z. Li, J. Lin and K. Xie, Applied Catalysis B: Environmental, 2015, 164, 18-30.
- 32 F. Hu, S. Tong, K. Lu, C.-M. Chen, F.-Y. Su, J. Zhou, Z.-H. Lu, X. Wang, G. Feng and R. Zhang, Journal of CO2 Utilization, 2019, 34, 676-687.
- 33 P. R. Yaashikaa, P. Senthil Kumar, S. J. Varjani and A. Saravanan, Journal of CO2 Utilization, 2019, 33, 131-147.
- 34 M. Nolan, ACS Omega, 2018, 3, 13117–13128.
- 35 Fisher Scientific, Magnesium Oxide, Heavy Powder, USP/FCC, Fisher https://www.fishersci.com/shop/products/ magnesium-oxide-heavy-powder-usp-fcc-fisherchemical-2/M68500.
- 36 Lab Alley, Calcium Oxide Powder, Lab Grade, https: //www.laballey.com/products/calcium-oxide-powderlab-grade.
- 37 I. Pełech, D. Sibera, P. Staciwa, E. Kusiak-Nejman, J. Kapica-Kozar, A. Wanag, U. Narkiewicz and A. W. Morawski, Materials, 2021, 14, 6478.
- 38 Sigma-Aldrich, Zinc Oxide, ReagentPlus®, Powder, ¡5 µm Particle Size, 99.9%, https://www.sigmaaldrich.com/US/en/ product/sigald/205532.
- 39 Sigma-Aldrich, Nickel(II) Oxide, 99.99% Trace Metals Basis, https:// www.sigmaaldrich.com/US/en/product/aldrich/203882.
- 40 J. Kockler, M. Oelgemöller, S. Robertson and B. D. Glass, Cosmetics, 2014, 1, 128-139.
- 41 Sigma-Aldrich, Titanium(IV) Oxide, Anatase, Powder, 99.8% Trace Metals Basis, https://www.sigmaaldrich.com/US/en/product/ aldrich/232033.
- 42 S. Deng, B. J. Jolly, J. R. Wilkes, Y. Mu, J. A. Byers, L. H. Do, A. J. Miller, D. Wang, C. Liu and P. L. Diaconescu, Nature Reviews Methods Primers, 2023, 3, 28.

- 113, 5322-5363.
- 23 N. H. Florin and A. T. Harris, Chemical Engineering Science, 2009, 64, 44 H. Takeda, K. Koike, H. Inoue and O. Ishitani, Journal of the American Chemical Society, 2008, 130, 2023-2031.
 - 45 J. Hawecker, J.-M. Lehn and R. Ziessel, J. Chem. Soc., Chem. Commun., 1983, 536-538.
 - 46 N. T. Padmanabhan, N. Thomas, J. Louis, D. T. Mathew, P. Ganguly, H. John and S. C. Pillai, Chemosphere, 2021, 271, 129506.
 - 47 A. Nosrati, S. Javanshir, F. Feyzi and S. Amirnejat, ACS Omega, 2023, 8, 3981-3991.
 - 48 O. Ola and M. M. Maroto-Valer, Appl. Catal. A: Gen., 2015, 502, 114–121.
 - 49 B. Yu, Y. Zhou, P. Li, W. Tu, P. Li, L. Tang, J. Ye and Z. Zou, Nanoscale, 2016, 8, 11870–11874.
 - 50 B. Michalkiewicz, J. Majewska, G. Kadziołka, K. Bubacz, S. Mozia and A. W. Morawski, J. CO2 Util., 2014, 5, 47-52.
 - 51 M. S. Akple, J. Low, Z. Qin, S. Wageh, A. A. Al-Ghamdi, J. Yu and S. Liu, Chinese J. Catal., 2015, 36, 2127-2134.
 - 52 Q. D. Truong, J.-Y. Liu, C.-C. Chung and Y.-C. Ling, Catal. Commun., 2012, **19**, 85-89.
 - 53 J. C. Wu, Catal. Surv. Asia, 2009, 13, 30-40.
 - 54 Q. Huang, J. Yu, S. Cao, C. Cui and B. Cheng, Appl. Surf. Sci., 2015, 358, 350-355.
 - 55 G. B. Damas, D. A. Ivashchenko, I. Rivalta and C. M. Araujo, Sustain. Energy Fuels, 2021, 5, 6066–6076.
 - 56 E. Jacob-Lopes, S. Revah, S. Hernández, K. Shirai and T. T. Franco, Chem. Eng. J., 2009, 153, 120–126.
 - 57 Sigma-Aldrich, Rhenium(III) chloride, powder, 61.4-65.9% Re, https:// www.sigmaaldrich.com/US/en/product/aldrich/309184, Accessed: 2024-09-04.
 - 58 Sigma-Aldrich, Ruthenium powder, 99.99% trace metals basis, https:// www.sigmaaldrich.com/US/en/product/aldrich/545023, Accessed: 2024-09-04.
 - 59 A. A. Olajire, Renew. Sustain. Energy Rev., 2018, **92**, 570–607.
 - 60 K. Sumida, D. L. Rogow, J. A. Mason, T. M. McDonald, E. D. Bloch, Z. R. Herm, T.-H. Bae and J. R. Long, Chem. Rev., 2011, 112, 724-781.
 - 61 Y. An, X. Lv, W. Jiang, L. Wang, Y. Shi, X. Hang and H. Pang, Green Chem. Eng., 2024, 5, 187–204.
 - 62 I. del Castillo-Velilla, A. Sousaraei, I. Romero-Muniz, C. Castillo-Blas, A. S. J. Méndez, F. E. Oropeza, V. A. de la Pena OShea, J. Cabanillas-González, A. Mavrandonakis and A. E. Platero-Prats, Nat. Commun., 2023, 14, 2506.
 - 63 H. Lyu, O. I.-F. Chen, N. Hanikel, M. I. Hossain, R. W. Flaig, X. Pei, A. Amin, M. D. Doherty, R. K. Impastato, T. G. Glover, D. R. Moore and O. M. Yaghi, J. Am. Chem. Soc., 2022, 144, 2387–2396.
 - 64 M. Songolzadeh, M. Soleimani, M. Takht Ravanchi and R. Songolzadeh, Sci. World J., 2014, 2014, 1-34.
 - 65 N. L. Rosi, J. Eckert, M. Eddaoudi, D. T. Vodak, J. Kim, M. OKeeffe and O. M. Yaghi, Science, 2003, 300, 1127-1129.

- 66 M. H. Beyzavi, C. J. Stephenson, Y. Liu, O. Karagiaridi, J. T. Hupp and O. K. Farha, *Front. Energy Res.*, 2015, **2**, year.
- 67 U. Ravon, M. Savonnet, S. Aguado, M. E. Domine, E. Janneau and D. Farrusseng, *Microporous Mesoporous Mater.*, 2010, 129, 319–329.
- 68 D. Sharma, S. Rasaily, S. Pradhan, K. Baruah, S. Tamang and A. Pariyar, Inorg. Chem., 2021, 60, 7794–7802.
- 69 T. Zelenka, K. Simanova, R. Saini, G. Zelenkova, S. P. Nehra, A. Sharma and M. Almasi, *Sci. Rep.*, 2021, **12**, year.
- 70 C. H. Hendon and A. Walsh, Chem. Sci., 2015, 6, 3674–3683.
- 71 Y. Zhang, H. Wang, X. Li, J. Chen and Z. Liu, *Carbon Research*, 2023, 2, 100060.
- 72 H. Dong, L. Li and C. Li, Chem. Sci., 2023, 14, 8507–8513.
- 73 U. Ryu, S. Jee, P. C. Rao, J. Shin, C. Ko, M. Yoon, K. S. Park and K. M. Choi, Coordination Chemistry Reviews, 2020, 426, 213544.
- 74 V. Gargiulo, F. Raganati, P. Ammendola, M. Alfe and R. Chirone, *Chem. Eng. Trans.*, 2015, 43, 1087–1092.
- 75 Helios SciTech, HKUST-1 (MOF-199), Cu-BTC MetalOrganic Framework, https://heliosscitech.com/product/hkust-1-mof-199-helios/, Accessed: 2025-09-20.
- 76 H. Takeda, H. Kamiyama, K. Okamoto, M. Irimajiri, T. Mizutani, K. Koike, A. Sekine and O. Ishitani, *Journal of the American Chemical Society*, 2018, 140, 17241–17254.
- 77 International Energy Agency, *Tracking Clean Energy Progress* 2023, https://www.iea.org/reports/tracking-clean-energy-progress-2023, 2023, Accessed: 2025-09-20.